

Secondary Controller for Voltage and Frequency Regulation in an Islanded Microgrid System Based on Anti-Windup Loop

Author

Mahmoudian, Ali, Garmabdari, Rasoul, Bai, Feifei, Stegen, Sascha, Lu, Junwei

Published

2022

Conference Title

14th IEEE PES Asia-Pacific Power and Energy Engineering Conference

Version

Accepted Manuscript (AM)

Rights statement

© 2022 IEEE. Personal use of this material is permitted. Permission from IEEE must be obtained for all other uses, in any current or future media, including reprinting/republishing this material for advertising or promotional purposes, creating new collective works, for resale or redistribution to servers or lists, or reuse of any copyrighted component of this work in other works.

Downloaded from

<http://hdl.handle.net/10072/418237>

Link to published version

<https://iee-appeec.org/>

Griffith Research Online

<https://research-repository.griffith.edu.au>

Secondary Controller for Voltage and Frequency Regulation in an Islanded Microgrid System Based on Anti-Windup Loop

Ali Mahmoudian*, Rasoul Garmabdari, Feifei Bai, Sascha Stegen, Junwei Lu

School of Engineering and Built Environment, Griffith University, Brisbane, Australia

*ali.mahmoudian@griffithuni.edu.au

Abstract—This paper presents an anti-windup (AW) proportional-integral (PI) secondary controller for both voltage and frequency restoration and stabilization for a stand-alone Microgrid (MG) system. The MG comprises four distributed generations (DGs) with distributed droop-based primary control systems and a centralized AW based secondary controller. The significance of this research is using a clamping model of the AW proportional-integral (AWPI) controller to suppress the possible overshoot or undershoot of the control signal during the secondary control operation and reduce the settling time of the PI controller. The suggested technique considers the voltage and frequency coupling in the stand-alone MG system. Some load and generation change scenarios are also modelled to approve the plug-and-play capability of this novel control fashion. In the end, the performance of the proposed control system is verified by using MATLAB®/SIMULINK software.

Keywords— *Microgrid, Hierarchical Control, Islanded, Anti-Windup*

I. INTRODUCTION

Renewable based Microgrids (MGs) can be the building block of the future of electricity networks. Consequently, in 2021, the Australian Renewable Energy Agency (ARENA) announced that the Australian Government would finance \$50 million in the MG pilot projects across Australia's regional area [1]. MG system can operate in two modes: grid-connected or islanded. In the remote areas, which are very common in Australia, the MGs usually work in the stand-alone mode to provide the power supply to their local customers. Therefore, it is crucial to maintain the voltage and frequency of the system within their acceptable margins.

The dynamic stability of droop control cannot adapt to different operating conditions of the MG. Thus, a hierarchical control system by adding a second level to the control system needs to be implemented to cope with this shortage [2]. Hence, the primary and secondary control levels are implemented to regulate the voltage and frequency of the system at the desired levels [3]. Abundant papers can be found in the literature on the hierarchical control structure of the MGs. Most conventional primary control methods, including droop control, master-slave, virtual impedance etc., were reviewed in [4]. Distributed secondary control in an unbalanced load condition with unequal reactive power was investigated in [5]. In both modes of MG operation, islanded and grid-connected, the secondary control is responsible for maintaining the system frequency and voltage within their respective permissible limits [6]. In [7], the performance and merits and drawbacks of the different control approaches such as Fuzzy logic controller, artificial neural network (ANN) controller,

proportional-resonant (PR), and conventional proportional-integral (PI) controller in voltage control of the MG have been thoroughly discussed. Authors in [8] proposed a method to use the redundant power capacity of a neighbour MG in a multi-MG (M-MG) system to maintain the voltage and frequency stability of an islanded MG. Some metaheuristic optimization algorithms like non-dominated sorting genetic algorithm II (NSGA-II) were considered in [9] to reduce the frequency deviations of a cluster of MGs. In [10] a Fuzzy-based secondary controller was developed to stabilize and control the voltage of an islanded MG. In the literature, some alternative secondary control methods such as multi-agent system and consensus-based algorithms were proposed to cope with the traditional PI controller weaknesses, such as not adaptable in load variation scenarios, low convergence speed, and control signal oscillation in voltage and frequency regulation [10]. However, using the anti-windup loop in the secondary PI controller can address these issues without adding more complexity to the control system since the anti-windup loop does not change the poles and zeros of the system. Therefore, the proposed method has several benefits, such as reducing the system overshoot/undershoot, decreasing the settling time of the under-control signal, and is less complex than the aforementioned control approaches.

The PI controller has been frequently used in the controlling process. Still, the performance of the conventional PI controller when dealing with some disturbances, i.e., load and generation changes and communication delays is not suitable [11]. As a result, its performance should be enhanced properly. The main contribution of this paper is proposing an adaptive anti-windup (AW) PI (AWPI) controller in the secondary level of the MG control system to suppress the voltage and frequency violations during different test scenarios in the network comprising four MGs with different nominal powers. The robustness of the proposed controller is investigated by considering the sudden change in the load.

The rest of the paper is organised as follows: An insight into the AWPI controller, details of the mathematical formulas of the primary control level and the AWPI secondary controller are proposed in Section II. In Section III, case study, simulation and results are presented. Lastly, Section IV concludes the paper.

II. PRIMARY CONTROL AND ANTI-WINDUP BASED SECONDARY CONTROL SYSTEM

In real-life, almost all the systems and processes are nonlinear and with upper and lower limitations. For instance, in frequency control of a MG, there is an acceptable operating margin for frequency, such as $\pm 1\%$ of the nominal frequency.

Hence, the control system should have a saturation block to emulate the system behaviour in real life. The control signal will be saturated when the actuator or the PI controller output gets saturated. Then it will remain in this condition leading to a break in the feedback. As a result, significant error accumulates, causing an overshoot or undershoot in the system. This problem is called wind-up [12]. Some approaches have been proposed to deal with this phenomenon in the PI controller, such as Back-Calculation and Clamping [13]. The Back-Calculation resets the integral part of the controller when a wind-up occurs. The integral part will be disabled when the controller output is saturated in the Clamping method. The conceptual representation of the AWPI is illustrated in Fig. 1.

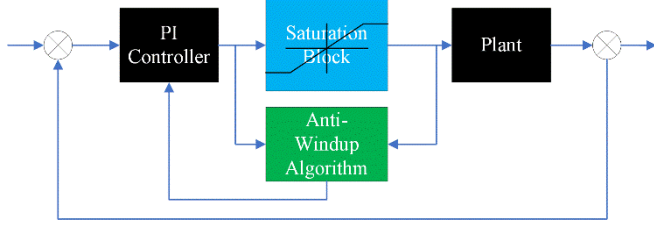


Fig. 1. Anti-Windup PI controller overall function.

The hierarchical control architecture comprises three levels. The primary level or the local controller of inverter-based MG tries to maintain the system voltage and frequency in their standard margins in the normal and continuous operation of MG, while the secondary controller's responsibility is to compensate the deviations caused by the primary controller, especially when an event (e.g., load changing, and generation curtailment) has occurred in the network. The tertiary control system manages the economic operation and optimal power flow between MGs and the grid [14]. In Fig. 2, the general outline of the hierarchical control system in islanded operating mode of MGs is depicted.

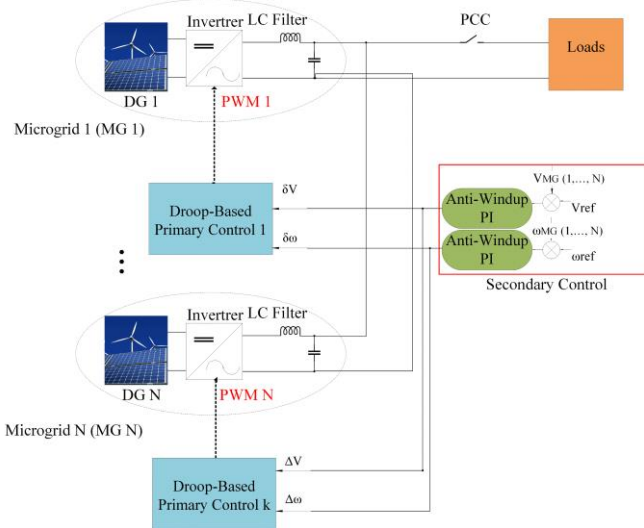


Fig. 2. Primary and secondary control levels in an islanded MG.

The following equations (1) and (2) formulate the secondary and primary controllers' mathematical models and correlations. At the primary level, the voltage and frequency of each MG are measured locally and then compared with the reference values of each of them. After that, this difference error passes through a PI controller to compensate for the deviations.

At the secondary level, the obtained voltage and frequency of each MG after the primary controller action are compared with the nominal values of the system ($V=400\text{ V}$ and $f=50\text{ Hz}$), and then the error signals go through the AWPI controller to regulate the voltage and frequency to the system's desired level.

$$\Delta\omega = K_{p\omega S}(\omega_{ref} - \omega_{MGk}) + K_{i\omega S} \int (\omega_{ref} - \omega_{MGk})$$

$$\Delta V = K_{pV S}(V_{ref} - V_{MGk}) + K_{iV S} \int (V_{ref} - V_{MGk}) \quad (1)$$

$$\omega_{Pr} = \omega_{ref} - m_{\omega k} (P_{calMGk} - P_{refMGk}) + \Delta\omega$$

$$V_{Pr} = V_{refMGk} - n_{vk} (Q_{calMGk} - Q_{refMGk}) + \Delta V \quad (2)$$

Where S and Pr denote the secondary and primary control levels. ref and cal abbreviate reference and calculated signals. Kp and Ki represent proportional and integral coefficients of PI controller, and $K=(1,2,\dots,N)$ is the number of MGs. Also, $m_{\omega k}$ and n_{vk} are droop coefficients for frequency and voltage control, respectively.

The main objectives of this paper is minimizing the voltage and frequency deviations of the system by implementing the droop based primary and AWPI based secondary controllers. The objective functions and their corresponding constraints are as follow:

$$\forall i \in N; \text{Min}(V_{devup} - V_{devlow})$$

$$\forall i \in N; \text{Min}(f_{devup} - f_{devlow}) \quad (3)$$

$$\text{While: } \forall i \in N; 0.95 \leq V_i \leq 1.05 \text{ p.u}$$

$$\text{and: } \forall i \in N; 0.994 \leq f_i \leq 1.006 \text{ p.u} \quad (4)$$

Where V_{devup} , V_{devlow} , f_{devup} , f_{devlow} are the voltage and frequency upper and lower levels deviations. N is number of MGs. V_i and f_i are the voltage and frequency of each MGs, respectively. According to IEEE STD 1547, the voltage margin bandwidth is $\pm 10\%$, and the frequency difference is $\pm 0.3\text{ Hz}$. But for this paper, the voltage deviation margin is limited to $\pm 5\%$ for better voltage regulation.

The flowchart for the proposed method is illustrated in Fig. 3.

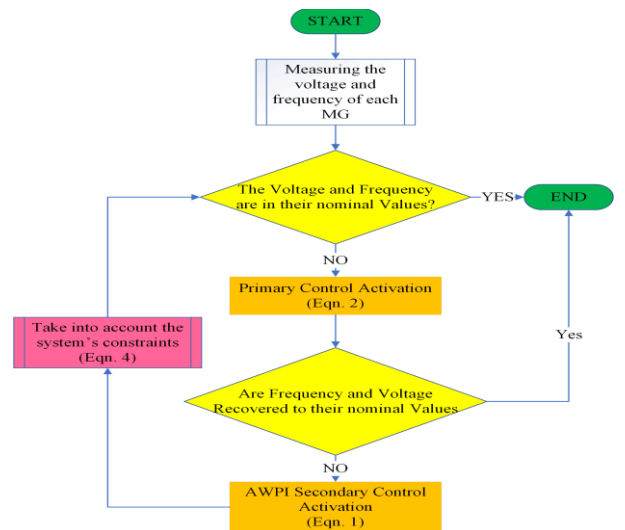


Fig. 3. The proposed control method flowchart.

In this paper, four inverter-based MGs connected to the point of common coupling (PCC) construct the study case. Multi Microgrid (MMG) can enhance the system's resilience, reliability, and flexibility levels and reduce the operation costs by feeding more external loads of other MGs. Also, there are four inverters in the Advanced Microgrid Lab of Griffith University for future system development, including experimental tests on the proposed system. Fig. 4 shows this network.

The specifications and ratings of the network are in the Table I. This study considers two static loads and one variable lumped load with 472 kVA, 75 kW, and 283 kVA apparent powers. Two static loads are connected to the PCC permanently, while the variable load which is considered as a lumped load represents total loads of some consumers that can be changed during the operation time of the system.

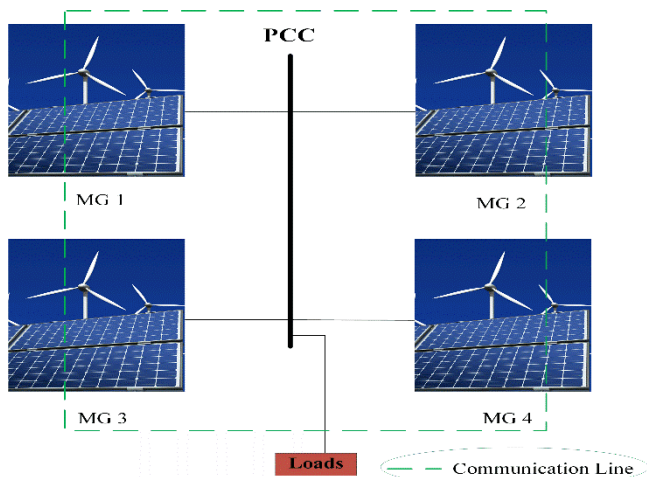


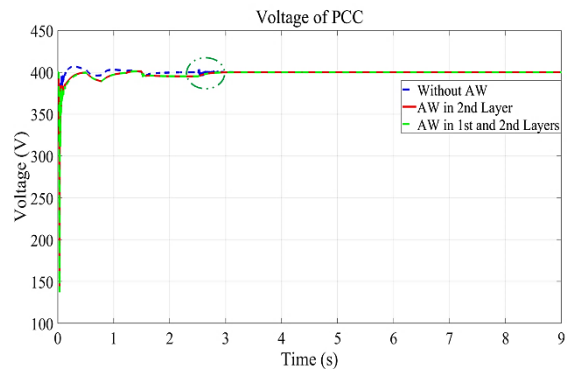
Fig. 4. Case study network.

TABLE I. MGs NETWORK CHARACTERISTICS

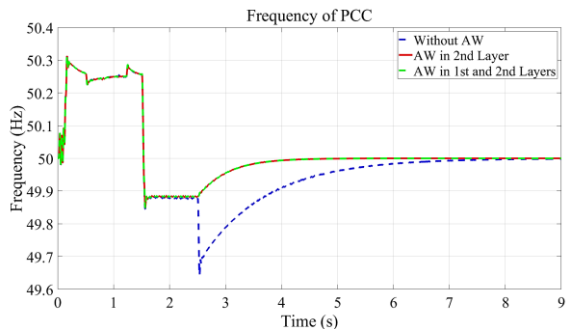
Parameter	Capacity	Unit
S_{MG1}	450	kVA
S_{MG2}	250	kVA
S_{MG3}	300	kVA
S_{MG4}	150	kVA
Voltage	400	V
Frequency	50	Hz

III. CASE STUDY AND RESULTS DISCUSSION

First of all, to verify the functionality of the proposed AWPI secondary controller, the MGs network is simulated in three different operation modes of the control system, including without AW loop, by AW loop in both primary and secondary controllers, and just AW loop in the secondary layer. Fig. 5 compares the performance of the hierarchical control system in these three different operation modes. In all simulation scenarios, at $t=0.5s$, the variable lumped load with a capacity of 283 kVA is connected to the network, while the static loads have been connected permanently. The primary and secondary controllers' trigger times are $t=1.5s$ and $t=2.5s$, respectively. As the system is starting and operating in islanded condition, some voltage and frequency deviation can be observed in the first milliseconds of the simulations.



(a). Voltage



(b). Frequency

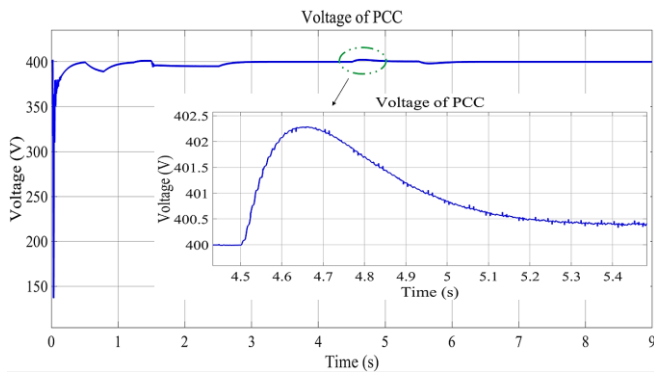
Fig. 5. Comparing AWPID controller performance in different layers of the hierarchical control system.

As shown in Fig. 5, embedding the AW loop in the secondary controller eliminates the overshoot or undershoot of the controlling approach, and the system stability is boosted by reducing the settling time of the voltage and frequency controllers. Besides, it can be inferred that the AW loop has more effects on lowering the undershoot in frequency terms. Besides, the AW loop's effectiveness on the secondary layer outweighs its performance on the primary level. So, the optimal approach is to embed the AW loop in the secondary layer of the control system. In the conventional PI controller-based frequency control, overshoot/undershoot will happen when the secondary layer control system is actuated [15]. It should be noted that the PI controller coefficients, i.e., K_p and K_i are tuned based on "Frequency Response" method.

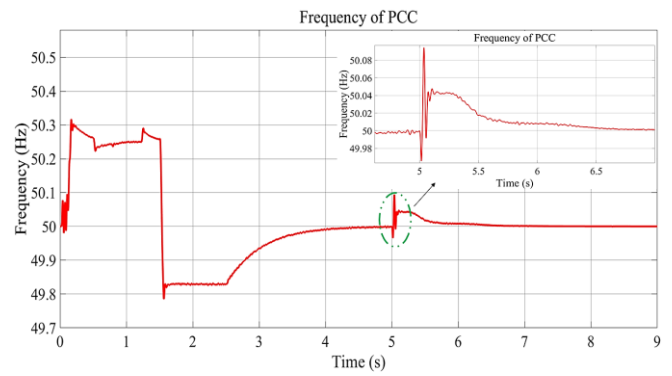
Two different scenarios are considered to investigate the efficiency of the proposed control system in recovering voltage and frequency of the MG system such as abrupt load variations and generation outage.

A. Sudden load reduction

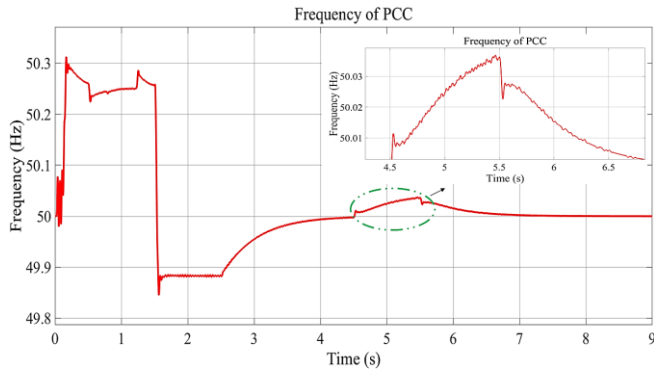
Load variation has adverse effects on the network's voltage and frequency stability. This impact may be more detrimental in an islanded MG, so designing and implementing a robust and autonomous control system to deal with this challenging condition is crucial. As mentioned in section 2, a bunch of customers' loads are considered as a variable lumped load. In order to evaluate the proposed control system performance in the load change conditions at $t=4.5s$, 283 kVA is deducted from the dynamic lumped load. The voltage and frequency profiles of the PCC are depicted in Fig. 6.



(a). Voltage



(b). Frequency



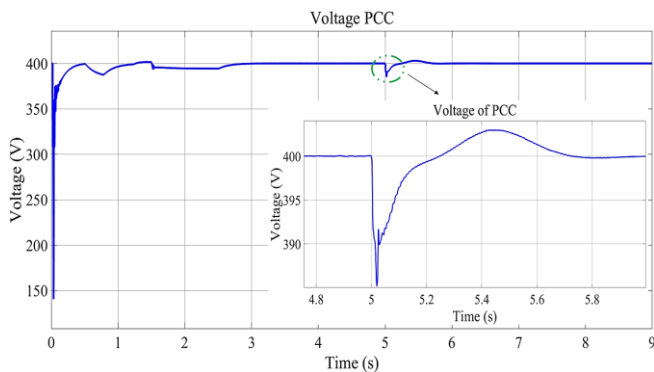
(b). Frequency

Fig. 6. The primary and secondary controllers' functionality as the load changes.

Fig. 6. shows that the control system can fully address the deviations happened due to the sudden load variations. It is worth mentioning that the voltage and frequency deviation at load disconnect time ($t=4.5s$) are at their corresponding permissible variation ranges, implying that the system operates in a stable condition during the transient time.

B. Generation curtailment

Sometimes a sudden fault or event in the electricity network may lead to the loss of a distributed generation (DG) unit. However, the control system should be robust enough to cope with any possible volatility. At $t=5s$, MG 4 is shut down, and all the variable and static loads should be supplied by the three remained MGs. The results of this scenario can be found in Fig. 7.



(a). Voltage

Fig. 7. Proposed control system performance in fault condition.

The above results verify the control system performance to regulate the voltage and frequency of the system when an incident like a generation outage occurs. Also, the same as in the previous scenario, the system's parameters are within their acceptable margins during the fault period.

To show the proposed control strategy capability to maintain the system voltage and frequency in the sinusoidal waveform in all three phases without distortion, the voltage and current of PCC are depicted in Fig. 8 and Fig. 9 for load changing scenario.

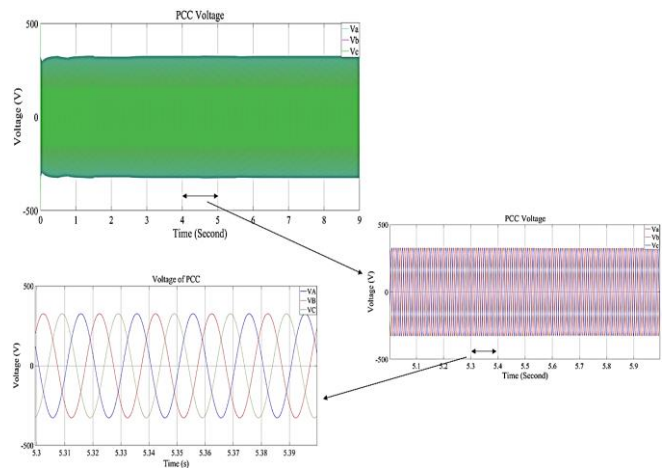


Fig. 8. PCC voltage waveform

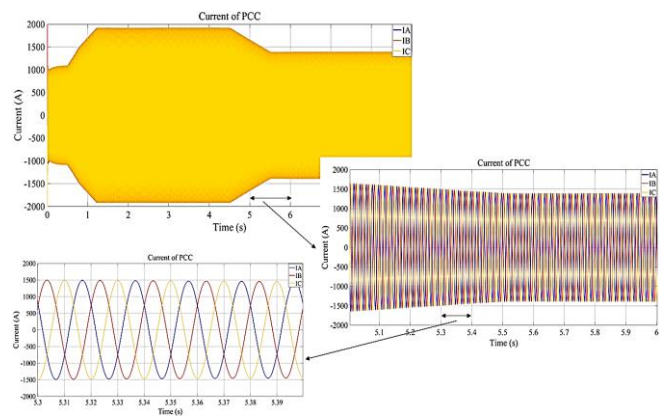


Fig. 9. PCC current waveform

As can be found from these figures, the voltage of the network has remained stable in all three phases during the control system's different operation stages, including the primary and the secondary control activation and load shedding. The

voltage and current waveforms between $t=5$ s and $t=6$ s (after load decrease) are presented for better understanding.

IV. CONCLUSION

This paper has presented an anti-windup hierarchical control approach to stabilize and control the voltage and frequency of networked microgrids under normal and abnormal network operating modes. The primary control is based on the conventional droop-based controller, and the AWPI controller creates the secondary control level aiming to regulate the deviations introduced by the primary controller. The obtained results have shown that using the AW loop in the primary control level does not bring any improvement or benefit for the whole control system; while embedding the AW loop in the secondary level of the hierarchical control system not only eliminates any possible overshoot or undershoot of the controlling process but also decrease the settling time of the system, which is important for the MG control system robustness and stability. In addition, different test scenarios such as load changing and generation sudden curtailment have been run to verify the proposed system functionality.

Future works will consider the unbalanced three-phase and single-phase load impacts on the control system, harmonic distortion level control in four-leg inverter-based MG, and neutral current control.

REFERENCES

- [1] "\$ 50 million to ramp up microgrids in regional Australia," no. SEPTEMBER, p. 2021, 2021.
- [2] Y. Han, H. Li, P. Shen, E. A. A. Coelho, and J. M. Guerrero, "Review of Active and Reactive Power Sharing Strategies in Hierarchical Controlled Microgrids," *IEEE Transactions on Power Electronics*, vol. 32, no. 3. Institute of Electrical and Electronics Engineers Inc., pp. 2427–2451, Mar. 01, 2017. doi: 10.1109/TPEL.2016.2569597.
- [3] Y. Zhang, L. Xie, and Q. Ding, "Interactive Control of Coupled Microgrids for Guaranteed System-Wide Small Signal Stability," *IEEE Trans. Smart Grid*, vol. 7, no. 2, pp. 1088–1096, 2016, doi: 10.1109/TSG.2015.2495233.
- [4] K. Ahmed, M. Seyedmahmoudian, S. Mekhilef, N. M. Mubarak, and A. Stojcevski, "A Review on Primary and Secondary Controls of Inverter-interfaced Microgrid," *J. Mod. Power Syst. Clean Energy*, vol. 9, no. 5, pp. 969–985, 2021, doi: 10.35833/MPCE.2020.000068.
- [5] A. Navas-Fonseca *et al.*, "Distributed Predictive Secondary Control for Imbalance Sharing in AC Microgrids," *IEEE Trans. Smart Grid*, vol. 13, no. 1, pp. 20–37, 2022, doi: 10.1109/TSG.2021.3108677.
- [6] R. Jackson *et al.*, "A comprehensive motivation of multilayer control levels for microgrids: Synchronization, voltage and frequency restoration perspective," *Applied Sciences* (Switzerland), vol. 10, no. 23. MDPI AG, pp. 1–30, Dec. 01, 2020. doi: 10.3390/app10238355.
- [7] K. A. Al Sumarmad, N. Sulaiman, N. I. A. Wahab, and H. Hizam, "Energy Management and Voltage Control in Microgrids Using Artificial Neural Networks, PID, and Fuzzy Logic Controllers," *Energies*, vol. 15, no. 1, Jan. 2022, doi: 10.3390/en15010303.
- [8] A. Arefi and F. Shahnia, "Tertiary controller-based optimal voltage and frequency management technique for multi-microgrid systems of large remote towns," *IEEE Trans. Smart Grid*, vol. 9, no. 6, pp. 5962–5974, Nov. 2018, doi: 10.1109/TSG.2017.2700054.
- [9] G. K. Suman, J. M. Guerrero, and O. P. Roy, "Stability of microgrid cluster with Diverse Energy Sources: A multi-objective solution using NSGA-II based controller," *Sustain. Energy Technol. Assessments*, vol. 50, Mar. 2022, doi: 10.1016/j.seta.2021.101834.
- [10] Q. Li, F. Chen, M. Chen, J. M. Guerrero, and D. Abbott, "Agent-Based Decentralized Control Method for Islanded Microgrids," *IEEE Trans. Smart Grid*, vol. 7, no. 2, pp. 637–649, 2016, doi: 10.1109/TSG.2015.2422732.
- [11] F. Kamal and B. Chowdhury, "Model predictive control and optimization of networked microgrids," *Int. J. Electr. Power Energy Syst.*, vol. 138, p. 107804, Jun. 2022, doi: 10.1016/j.ijepes.2021.107804.
- [12] B. G. K. Shantharam and P. Vidya, "Observer - based anti - windup robust PID controller for performance enhancement of damped outrigger structure," *Innov. Infrastruct. Solut.*, 2022, doi: 10.1007/s41062-022-00798-9.
- [13] L. R. da Silva, R. C. C. Flesch, and J. E. Normey-Rico, "Analysis of Anti-windup Techniques in PID Control of Processes with Measurement Noise *," *IFAC-PapersOnLine*, vol. 51, no. 4, pp. 948–953, 2018, doi: 10.1016/j.ifacol.2018.06.100.
- [14] J. M. Guerrero, J. C. Vasquez, J. Matas, L. G. De Vicuña, and M. Castilla, "Hierarchical control of droop-controlled AC and DC microgrids - A general approach toward standardization," *IEEE Trans. Ind. Electron.*, vol. 58, no. 1, pp. 158–172, 2011, doi: 10.1109/TIE.2010.2066534.
- [15] H. Tu, Y. Du, H. Yu, A. Dubey, S. Lukic, and G. Karsai, "Resilient information architecture platform for the smart grid: A novel open-source platform for microgrid control," *IEEE Trans. Ind. Electron.*, vol. 67, no. 11, pp. 9393–9404, 2020, doi: 10.1109/TIE.2019.2952803.